32nd Electric Vehicle Symposium (EVS32)
Lyon, France, May 19 - 22, 2019

Super Capacitor electrical and lifetime model development for low frequency current applications

Mahdi Soltani[1,2], Joris Jaguemont[1,2], Ahmed Abdallh[2], Omar Hegazy[1,2], Peter Van den Bossche[1,2], Joeri Van Mierlo[1,2], Noshin Omar[1,2]

[1]*Department ETEC Mobility, Logistics and Automotive Technology Research Group (MOBI), Vrije Universiteit Brussel, Pleinlaan 2, 1050 Brussels, Belgium, mahdi.soltani@vub.be*

[2] *Flanders Make, Gaston Geenslaan 8, 3001 Heverlee, Belgium*

Summary

The application of Super Capacitors (SCs) as an energy storage system covers a broad range of applications from transportation to stationary applications. There are also a variety of applications in which SC are used as an energy damper like in a textile industry which SC can be used to store the reciprocating energy from the weaving-loom machines for the next forward movement in order to improve the efficiency of the system. In this research, a commercial SC has been studied for lifetime expectation in such kind of application. An Extended Kalman Filter (EKF) electro-lifetime model is developed and validated. The result shows that in this alternative current application, the lifetime is much less than the nominal conditions due to the low frequency effect. An error of less than 2% proves the accuracy of the proposed model. With this ageing model, the lifetime can be examined, and the best utilization profile can be designed to ensure the SC safety and lifetime extension

Keywords: extended Kalman filter, frequency effect, lifetime modelling, SoC estimation, supercapacitor

1 Introduction

Supercapacitors (SCs), also called electrochemical double layer capacitors (EDLCs), are energy storage systems (ESSs), suitable for high power applications over a wide range of temperature and with a very long cycle life. These characteristics make SCs desirable for high cyclability in different applications such as textile industry where fast motion weaving machines exchange energy with the power source frequently. In such kind of applications, the energy is exchanged between the weaving machine and energy storage at a low frequency in the order of 5 to 15 Hz. In order to design a proper energy storage system for this kind of application, the effect of low frequency current waveform on the lifetime of the SC need to be investigated.

Studies available in the literature on the lifetime of SC focus either on the floating constrains (constant voltage and temperature) and very low frequency (<1 Hz) high current cycles [1] or on a very high frequency (few kHz) current ripples generated by choppers [2]. However, the effect of medium frequency currents on the lifetime of SC has not been studied yet.

The SC used in the stationary or transportation applications is characterized of having a useful life defined by the number of continuous charge-discharge cycle with respect to a certain value of capacity fade and internal resistance raise. The selected SC in this study, according to the datasheet provided by the manufacturer, is reported by having a remaining capacity of 90% after 1.5 million cycles at a current rate of 500A peak to peak at 25°C with 30 seconds rest between each cycle. In other word, after each cycle, the coulombic capacity of the SC reduces. In alternative current (AC) applications, the low coulomb charge and discharge cycles may also have effect on the useful lifetime of SC as it produces repeated columbic charge-discharge cycles. Electrochemical Impedance Spectroscopy (EIS) method has also revealed that both the active (ohmic) and reactive component of the SC are dependent to the frequency indicating that frequency also affects the lifetime of the SC [3].

Recently, Uno and Tanaka [4] have studied the lifetime performance of a selected LiB when it is subjected to an AC current at the frequency range of 1 Hz to 100kHz. The author has employed a single AC current at a very low amplitude without DC offset. This means that the tests were carried out around a single SoC and therefore at a single voltage. The results show that the cell cycles at frequencies above 10Hz has a similar degradation trend as calendar aging. Conversely, the cell cycled with a low frequency current waveform (less than 10Hz) has a deteriorated performance. A possible explanation for this result may be due to the time constant associated to the double layer capacitance and charge transfer resistance in the anode and cathode. As the time period of high frequency cycles are significantly shorter than RC time constant of the double layer capacitor, the sluggish charge transfer dynamic of the LiB does not have enough time to respond to the current disturbance. The same behavior has been reported for Lead-acid batteries [5] concluding that high frequency current fluctuations only charge and discharge the double layer capacitor and the ionic diffusion cannot happen. Equivalent circuit models presented in [4] also reveals that at high frequencies, the charge transfer resistance R_c is bypassed since most of the current flows through the lower capacitive resistance of X_c. It is noteworthy to say that the heat generation in the cells is due to current flowing through the R_c component. In high frequency current applications, the R_c component is bypassed by the X_c component, as a result the resistive loss will be negligible, and consequently the degradation trend mimics the calendar degradation.

The effect of high frequency current on the lifetime of SC also has been studied in many literatures. German et al. [2] studied the influence of hybrid vehicles high frequency current ripples (1 kHz) on the SC aging. The authors measured the impedance parameters evolution to monitor the SC state of health. The results show that the current ripples have a significant effect on SC aging kinetics and reliability. It is revealed that the package is failed due to the overpressure induced by high frequency current ripples. In this analysis, the authors proposed two possible explanations on the origin of overpressure. First, the overpressure could be caused by a gas overproduction because of the current ripple frequency. Second, the gases produced during floating are adsorbed in carbon activated structure. When gases are desorbed and liberated out of the porosity, they participate to the pressure increase inside the SC package. Venet et al. in [3] revealed that the 100Hz and 10kHz frequency does not have any effect on the lifetime of SC. It can be assumed that there is a frequency threshold for SC acts like a resonance frequency which intensifies the aging of the cell. The reasons behind this behavior is not yet fully understood but evidently this frequency level differs for each technology.

Uddin et al. in [6], have shown that the effect of high frequency current waveform is negligible if they are applied to the cell without a DC offset. In other word, the degradation rate considerably increases with the increase of current frequency for a cell cycled with a coupled AC-DC signal; however, the reason behind this behavior has not been explained and the frequency threshold in this condition has not been determined.

As summarized, the effect of low frequency currents on the lifetime of SC has been rarely studied in the academic literatures. In this research, an electrical and lifetime model for a commercial SC (1200F DLCAP) is studied. A real-life weaving-loom machine load profile is applied to the selected SC to study the effect of a low frequency (12 Hz) sinewave with high amplitude (80A peak to peak) on the lifetime. Finally, the end of life is estimated based on the proposed model and a possible solution for lifetime extension is proposed.

This paper is structured as follows: SC application is briefly explained in section 2. The principle of using SC as storage device in the considered applications is given in section 3. The electrical modeling principle and test procedure including the characterization method is explained in section 4. Within section 5 the lifetime model is presented. Simulation results and discussion are given in section 6, and finally the conclusions are drawn in section 7.

2 SC application in this study

Manufacturing machines often exhibit significant energy flows converted back and forth between the electrical and mechanical domain. In such manufacturing machines, the motion frequency is rather fast typically between 5 and 15 Hz for weaving-loom machines. Compared to the 'slow' energy storage of elevators and cranes, these kinds of applications exhibit a much higher power to energy ratio. Basically, there are several ways to store this energy [7]. Using an active front end, i.e. bidirectional power electronics converter, allows to feed the energy back to the grid, however it is a bit expensive solution and requires a complex control. Another option is to store the energy in a mechanical storage device, such as a flywheel or mechanical spring, which have limited lifetime and storage capability. Lastly, it is possible to store the energy electrically at the dc-bus in super capacitors, however the lifetime is a questionable in such applications.

In this paper, we aim at investigating the use of the SCs as electric storage devices when the reciprocating energy needs to be stored at the dc-bus. The considered topology is shown in Figure 1, where the load is a representative of a manufacturing machine, i.e. the four-bar linkage mechanism [8]. The load is connected to the grid terminals via line inductors and passive front end, i.e. uncontrolled three phase rectifier circuit. The capacitor bank consists of several series SC cells are used at the dc bus as shown in the Figure 1.

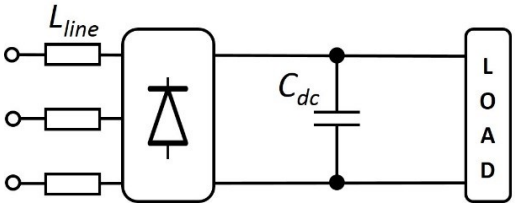

Figure 1: Schematic diagram of the use of super capacitors in manufacturing machine applications.

3 Super capacitor aging principals

SCs are composed of activated carbon nanopores electrodes facing each other in ionic saturated electrolyte. The electrodes are porous to maximize the contact surface with electrolyte which result in a high capacitance value. Collectors are used to electrodes with external circuit. Energy is stored by the double layer effect, i.e. one ionic charge facing one electronic opposite charge. During ageing, the electrolyte molecules (solvent and ions) react with parasitic surface groups (oxygenated groups remaining from the carbon activation) which modify the SC electrode. Specific surface of electrode is reduced by ageing reactions which produce solids and gases (capacitance decrease). These gases can be adsorbed on activated carbon or liberated out the porous structure creating a pressure increase which degrades electrodes (resistance increase) [2].

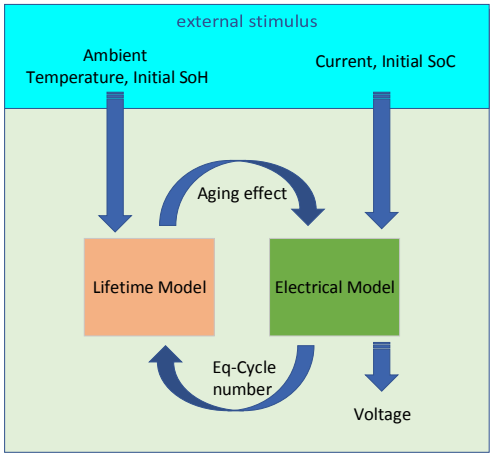

Figure 2: Model components and their interaction

4 Model components

The proposed electrical model for SC as shown in Figure 2 is presented in this section. The model is composed of two interconnected sub-models:

- Electrical model: predicts the SC terminal voltage and SoC as a function of ripple current. The output is influenced by initial temperature and initial SoC;
- Ageing model: predicts the capacity fade and resistance increase as a function of cell operating conditions such as SoC, temperature, charging/discharging current rate and cycles number.

4.1 Electrical sub-model

A SC voltage behaviour can be simulated by an Equivalent Circuit Model (ECM), which attempts to predict the voltage evolution of a SC using only electrical components. The structure of electrical model needs to be carefully chosen considering both the estimation accuracy and computational cost. Different types of ECM models have been developed in the last decades [9]–[11], among which the first order and second order electrical model are the most commonly used models thanks to their simplicity and reasonably good accuracy.

In this work, a 1st order Thevenin model as shown in Figure 3-a is used due to the linear voltage behaviour of SC [12]. This model is composed of a voltage source (V_{ocv}), an internal resistance (R_O) and one RC branch including the polarization resistance (R_P) and the charge transfer impedance (C_P). The I_L is the load current and V_t is the cell terminal voltage [13][14]. The electrical behaviour of the first order model can be described by Equations (1) and (2)[14]:

$$\dot{V}_{cp} = -\frac{V_{cp}}{R_P C_P} + \frac{I_L}{C_P} \tag{1}$$

$$V_t = V_{ocv} - I_L R_O - I_{RP} R_P \tag{2}$$

Experimental results reveal that the hysteresis effect (different charge and discharge behaviour) cannot be neglected in the model therefore, an adapted 1st order Thevenin model with the consideration of hysteresis effect has been used to simulate the SC's electrical behaviour during operations as shown in Figure 3-b. All parameters are dependent on the operating conditions (i.e., current, temperature, and SoC). The SoC is determined based on Extended Kalman Filter (EKF) [10].

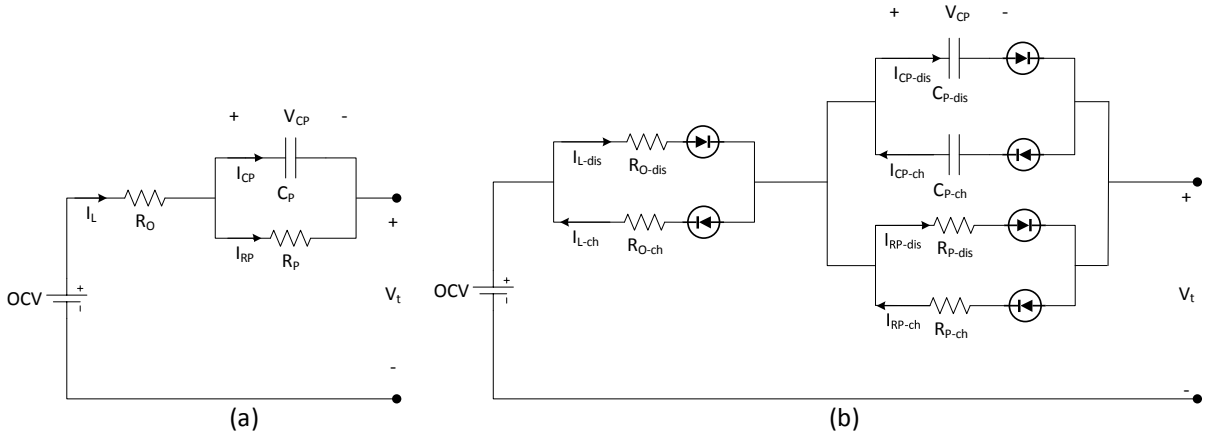

Figure 3: 1st order Thevenin model (a), Advanced 1st order Thevenin model (b)(adapted from [15])

4.1.1 Kalman filter theory

In order to understand the developed SoC estimator model based on Extended Kalman Filter, the theory of linear Kalman filtering is explained.

Figure. 4 represents a linear discrete time system, where A_k, B_k and C_k are time-varying matrices, $z^{-1}I$ is a unit delay block, u_k and y_k are the input and output of the system respectively, w_k represents the process

noise and v_k represents the noise on the measurement. x_k is the state of the system, which cannot be directly measured.

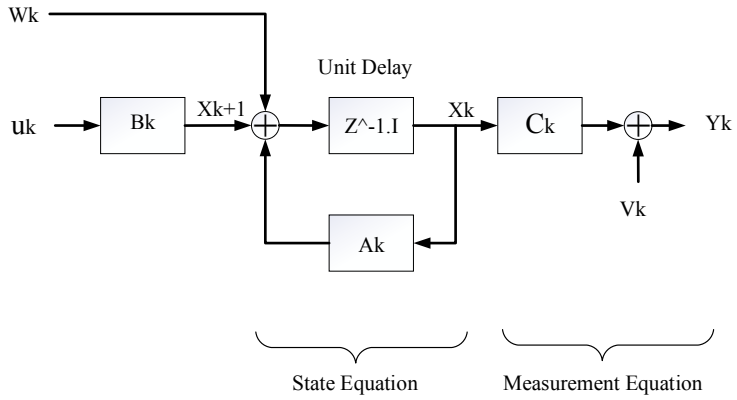

Figure 4: Schematic representation of Linear Discrete Time System [16]

To describe the system shown in Figure 4, the following two equations can be used [16]:

$$x_{k+1} = A_k x_k + B_k u_k + w_k \quad (3)$$

$$y_k = C_k x_k + v_k \quad (4)$$

where x_k is the state of the system at time k. This state can be a single variable or a vector of multiple variables like SoC and different voltages. y_k represents the output of the Kalman filter, generally the terminal voltage of the SC. u_k represents the input, which can also be a single variable or a vector (current, temperature, capacity, etc).

Equation 3 is the state equation of the system, describing the system dynamics. Equation 4 is the output equation, describing the output of the system as a linear combination of system states. The Kalman filter theory offers a solution to the following problem: using measured data u_k and y_k find the best estimate $\hat{x}_k$ of the true state x_k . This solution is a set of recursive equations that are widely accepted and available in the literature, which are shown as below [17]:

$$\bar{x}_{k+1} = A_k \hat{x}_k + B_k u_k \quad (5)$$

$$P_{k+1} = A_k \hat{P}_k x_k^T + Q_k \quad (6)$$

$$K_k = \bar{P}_{k+1} C_k^T [C_k \bar{P}_k C_k^T + R_k]^{-1} \quad (7)$$

$$\hat{x}_{k+1} = \bar{x}_{k+1} + K_k [y_k - \bar{y}_k] \quad (8)$$

$$\hat{P}_{k+1} = \bar{P}_{k+1} - K_k C_k \bar{P}_{k+1} \quad (9)$$

where the vector with an over-line (e.g. $\bar{x}$) indicates the prior estimation and with caret indicates (e.g. $\hat{x}$) the posterior estimation. Equation 5 and 6 represent the state of the system and the error covariance that are predicted for the next time step, respectively. The Kalman gain (K_k) is calculated in Equation 7, the Kalman gain determines the accuracy of the prior state estimation and error covariance estimation. When the prior state estimation and error covariance estimation are very trust-worthy, the Kalman gain will be small and thus result in a small update of the prior estimations in Equation 8 and 9. If the uncertainty on the prior estimation is large, the Kalman gain will be large thus resulting in a large update of the prior estimates.

4.1.2 Parameters estimation

In order to estimate parameters of the first order ECM (Figure 3), some experiments including OCV test, capacity check and Hybrid Pulsed Power Characterization (HPPC), as shown in Figure 5, have been performed at different current rates, different temperature and at different SoC levels. Using the least square fitting technique, those parameters have been extracted and have been stored into lookup tables. Table l shows a sample of extracted value from HPPC charge pulses for $R_{p\text{-}ch}$.

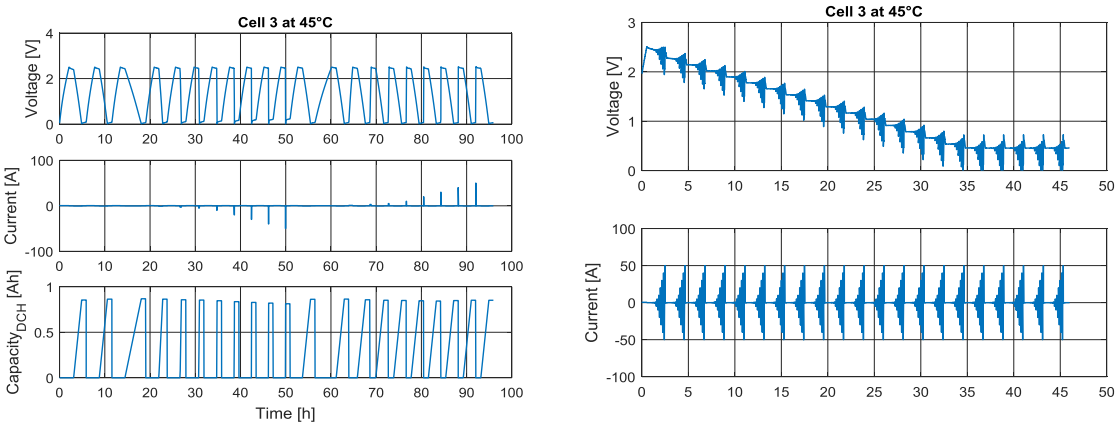

Figure 5: Capacity and HPPC tests performed @ 45°C

Table 1: some of the Rp-ch values extracted from HPPC test

SoC	Current (A)									
	0.24	0.48	1	3	5	10	20	30	40	50
0	0.000712	0.000727	0.00071	0.000796	0.000733	0.003629	0.001408	0.001132	0.001399	0.000712
50	0.013366	0.011354	0.005598	0.017689	0.009538	0.013115	0.016316	0.008241	0.009659	0.013366
100	0.05331	0.018287	0.046692	0.0505	0.047919	0.045051	0.045766	0.05696	0.05703	0.05331

4.2 Ageing sub-model

4.2.1 Capacity fade

Various research works have been carried out on both calendar and cycle ageing of EES with the empirical approach [18]. The SC cycle life is closely related to the operating conditions. The cycle number is mainly used as time notion for cycle life-time modelling. In some lifetime model, the Ah-throughput is calculated for cycle number calculation [19]. For most cells reported in the available literatures, the capacity loss shows power law relationship with cycling time or number, as shown in below:

$$Q_{loss}^{cyc} = A_{cyc} f(DoD, T, I) L^{z_{cyc}} \qquad (10)$$

As it is already known, the degradation of a SC cell is caused by a multiple ageing process in parallel and the effect of every ageing mechanism on each other makes the whole degradation process complicated. As shown in Figure 7, the capacity loss shows power law relationship with cycling time or numbers, this indicates that the SC ageing process is similar to the other storage systems despite their different technology. By using the experimental result shown in Figure 7 and extrapolation, the maximum number of cycles in which the capacity falls to the 80% of the initial capacity can be estimated. With the capacity fade estimation model, it is possible to size the storage system prior to the implementation to real applications.

4.2.2 Resistance growth

The internal resistance also increases as the cell is aged (Figure 9). The increase of the internal resistance can affect the output voltage of the cell as well as the power capability and storage capacity. According to the literature, the end of life is defined when the internal resistance increases 200% above the initial value.

5 Lifetime model construction

In this research work, a semi-empirical lifetime model for SC cells for low frequency applications is presented. After extracting all parameters shown in Figure 3, the model is implemented in MATLAB/Simulink software.

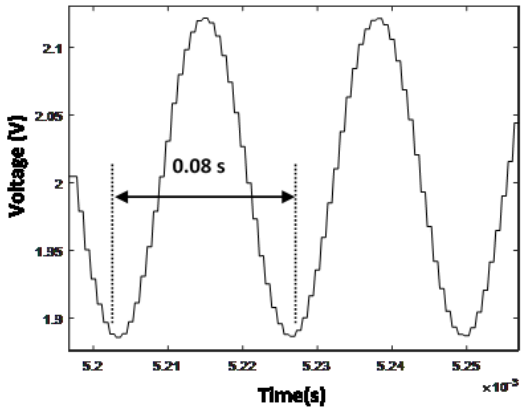

Figure 6: sinewave applied to the cell to study the frequency effect on lifetime

5.1 Experimental results

The ageing tests were carried out at 25 and 40°C temperatures, and all the cells were cycled with the sinusoidal current wave (40A-amplitude with 12 Hz frequency) at 80% SoC. In this experiment, the CT0550 PEC tester has been used and cells were placed in two temperature chambers at 25 and 45 degrees. The voltage variation is shown in Figure 6. The capacity test and internal resistance characterization are done during the experiments after every 700KCycles and the obtained results are stored in look up tables. The characterizations tests are performed at 28A, the RMS value of sinusoidal current wave.

Charge and discharge capacity degradation trends at both temperatures are shown in Figure.7. The trend shows the bigger impact of higher temperature on the capacity degradation. The impact of sinewave current on the capacitance and resistance parameters presented in Figure 3 is shown in Figures 8 and 9. It is evident that cycling at low frequency does not have a huge effect on the capacitance while the effect on the resistance is quite significant. It is also evident that the SoC does not have a large impact on the evolution of internal resistance while it has a considerable effect on the capacitance. According to [5] a bigger capacitance tends to a larger time constant for the double layer capacitor. Meaning that at higher voltage, SC will be less sensitive to the frequency than at lower voltages.

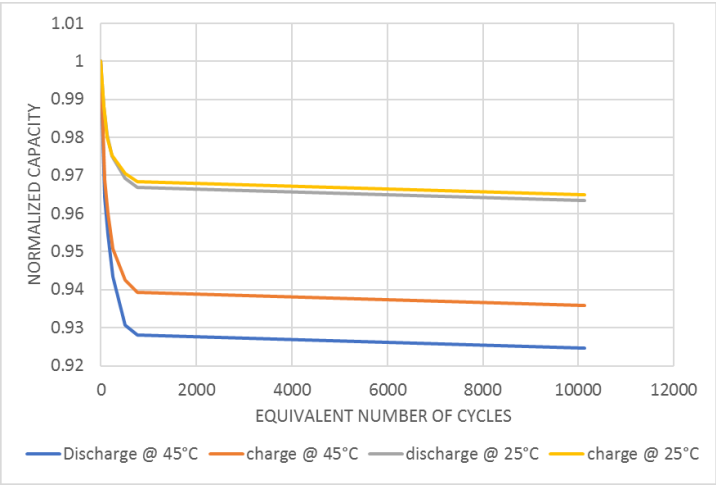

Figure 7: Capacity degradation at different temperature.

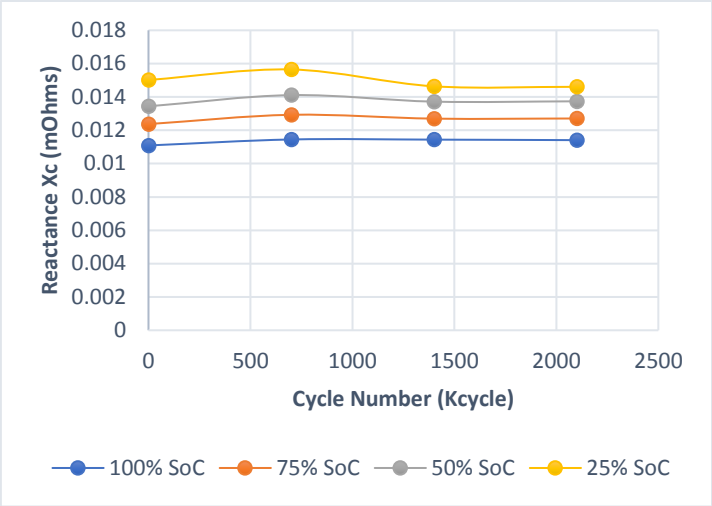

Figure 8: Reactance (Xcp) evolution at frequency of 10mHz and different voltage.

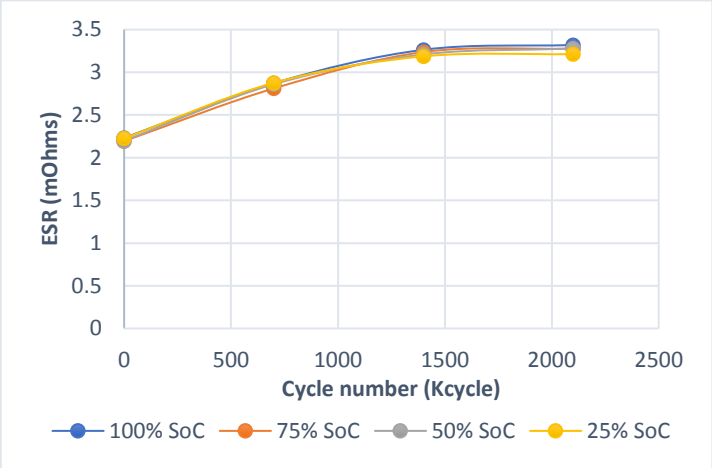

Figure 9: ESR (RO + Rp) evolution at frequency of 10mHz and different voltage

5.2 Model construction

As the capacity fades with the effect of cycle number and temperature, a Capacity Correction Factor (CCF) is introduced to determine the remaining usable SC capacity after a certain number of cycles. The CCF and remaining usable capacity can be defined by (11) and (12):

$$CCF = 1 - Q_{loss} \tag{11}$$

$$Q_{usable} = Q_{initial} \times CCF \tag{12}$$

This type of model is based on the capacity fade trend stored in look-up tables. Interpolation and extrapolation techniques are used to calculate the incremental capacity fade based on the equivalent number of cycles and updates the values of the SC capacity by providing the values of the capacity correction factors. The equivalent number of cycles is calculated by measuring the amount of discharged energy during the cycling test and dividing to the nominal available capacity of a fresh cell. The resistance growth and all parameters described in section 2 are updated based on the stored data in the look-up tables and extrapolation methods. Figures 10 and 11 show the interface of the proposed model in this research.

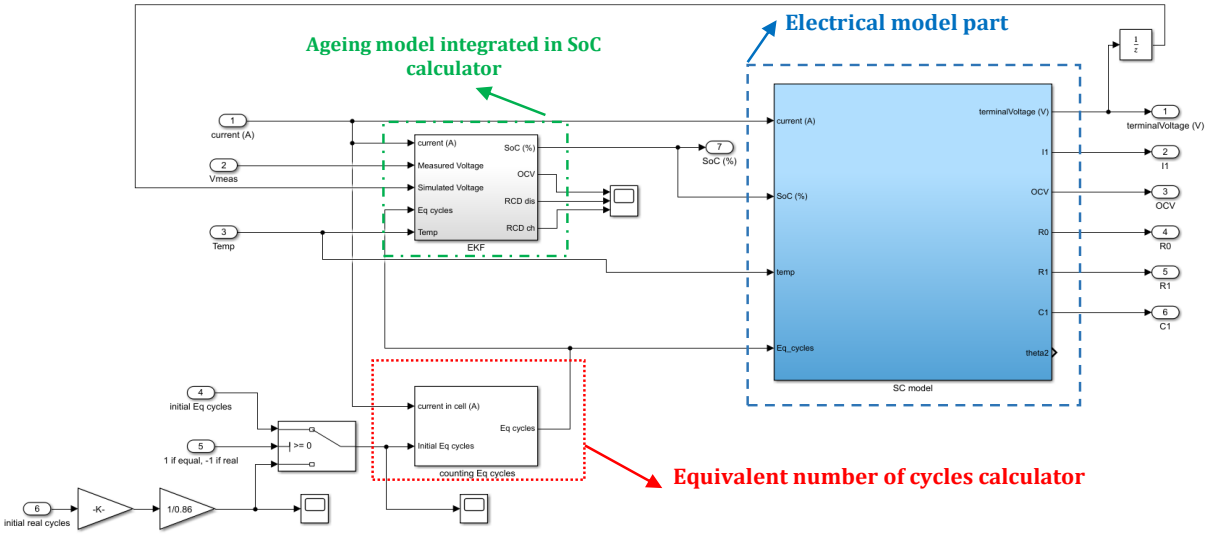

Figure 10: Interface of the developed 1st order electro-lifetime model

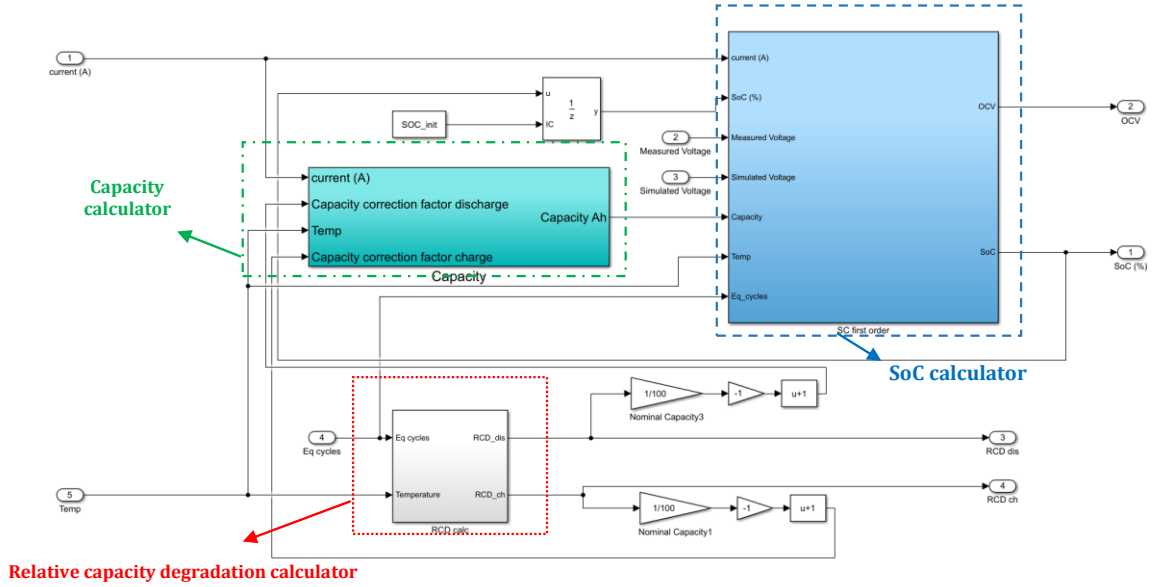

Figure 11: Interface of the aging model and SoC calculator.

6 Simulation result and discussion

For validation purpose, a dynamic load profile has been used. The simulated result has been compared with the experimental result as shown in Figure 12. The final estimation error is about 2% which proves the good accuracy for the proposed ageing model.

The simulation error can be calculated as:

$$error\% = 100\% \times \frac{V_{measured} - V_{simulated}}{V_{measured}} \qquad (13)$$

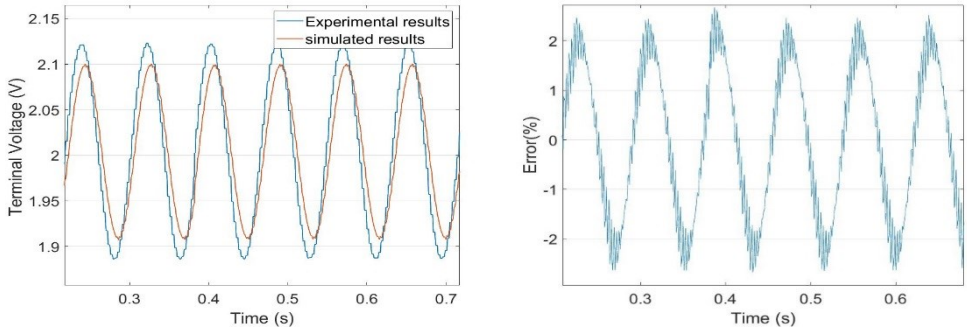

Figure 12: (a) Comparison of voltage response from cell 1 after 2.1 million sinewave cycles under a real load profile between experimental and simulated data (b) corresponding simulation errors

Using this model, the end of life is predicted at 600 thousand nominal cycles or 200 million sinewave cycles. Comparing to the expected cycle life presented by the manufacturer, it is evident that this cycling condition accelerates the aging process about four times faster than nominal cycling condition.

7 Conclusion

In this study, commercial SC cells were cycled under sinusoidal cycling wave at 25 and 40°C temperature. This study provides general information about the working and ageing behavior of SC and their degradation process. The developed first order lifetime model is based on EKF SoC estimation technique. The parameters of the proposed model were generated from the results of extended SC characterization tests.

The ageing test result shows that the cell capacity fade follows a power law relationship with the cycle numbers, while the power capability is also influenced throughout the cycle aging.

The dependency of the model parameters on SoC is investigated for cells at different ageing states and temperatures. The variation of parameters was considered during the ageing model development. Later, a more accurate estimation for the electrical behavior of the energy storage system is proposed to simulate the ageing state of the SC. A real load profile was used to validate the SC working performance. The error of about 2% proves a good accuracy for the developed ageing model. With this ageing model, the operating behaviors of this SC can be well presented. This research results can assist further life-time estimation modeling studies and helps the best applications selection for SC. Based on the analysis presented in this paper, SCs are not recommended in such kind of applications due to the fast degradation process because of the low frequency current waves.

Acknowledgments

We acknowledge Flanders Make for the grant provided for this research project. This work is performed as part of the PROFENSTO project, funded by the Institute for the Promotion of Innovation through Science and Technology in Flanders (VLAIO), Belgium. We also acknowledge Bluways company for supplying the SC cells for free for this research project.

References

[1] O. Briat, J. M. Vinassa, N. Bertrand, H. El Brouji, J. Y. Delétage, and E. Woirgard, “Contribution of calendar ageing modes in the performances degradation of supercapacitors during power cycling,” *Microelectron. Reliab.*, vol. 50, no. 9–11, pp. 1796–1803, 2010.

[2] R. German, O. Briat, A. Sari, P. Venet, M. Ayadi, Y. Zitouni, J.M. Vinassa, “Impact of high frequency current ripple on supercapacitors ageing through floating ageing tests,” Microelectron. Reliab., vol. 53, no. 9–11, pp. 1643–1647, 2013.

[3] P. Venet, O. Briat, A. Sari, J.-M. Vinassa, and R. German, “Study on specific effects of high frequency

ripple currents and temperature on supercapacitors ageing," *Microelectron. Reliab.*, vol. 55, no. 9–10, pp. 2027–2031, 2015.

[4] M. Uno and K. Tanaka, "Influence of high-frequency charge-discharge cycling induced by cell voltage equalizers on the life performance of lithium-ion cells," *IEEE Trans. Veh. Technol.*, vol. 60, no. 4, pp. 1505–1515, 2011.

[5] R. F. Nelson and M. A. Kepros, "AC ripple effects on VRLA batteries in float applications," pp. 281–289, 2008.

[6] K. Uddin, A. D. Moore, A. Barai, and J. Marco, "The effects of high frequency current ripple on electric vehicle battery performance," *Appl. Energy*, vol. 178, pp. 142–154, 2016.

[7] B. Lenaerts, A. Abdallh, D. Maes, B. Mrak, T. Galle, and W. De Waele, "Total Cost of Ownership Optimization of Manufacturing Machines with Fast Energy Storage," *Proc. - 2018 IEEE 18th Int. Conf. Power Electron. Motion Control. PEMC 2018*, pp. 784–789, 2018.

[8] G. S. McCarthy, J. Michael, Soh, *Geometric Design of Linkages*, 2nd ed. Springer-Verlag New York, 2011.

[9] D. Torregrossa, M. Bahramipanah, E. Namor, R. Cherkaoui, and M. Paolone, "Improvement of dynamic modeling of supercapacitor by residual charge effect estimation," *IEEE Trans. Ind. Electron.*, vol. 61, no. 3, pp. 1345–1354, 2014.

[10] L. Zhang, Z. Wang, F. Sun, and D. G. Dorrell, "Online parameter identification of ultracapacitor models using the extended Kalman filter," *Energies*, vol. 7, no. 5, pp. 3204–3217, 2014.

[11] R. A. Dougal, L. Gao, and S. Liu, "Ultracapacitor model with automatic order selection and capacity scaling for dynamic system simulation," *J. Power Sources*, vol. 126, no. 1–2, pp. 250–257, 2004.

[12] X. Hu, S. Li, and H. Peng, "A comparative study of equivalent circuit models for Li-ion batteries," *J. Power Sources*, vol. 198, pp. 359–367, 2012.

[13] R. E. W. S. Santhanagopalan, J. Stockel, "Secondary batteries-lithium rechargeable systems-lithium-ion|lifetime prediction," pp. 522–538, 2009.

[14] H. He, R. Xiong, and J. Fan, "Evaluation of lithium-ion battery equivalent circuit models for state of charge estimation by an experimental approach," *Energies*, vol. 4, no. 4, pp. 582–598, 2011.

[15] N. Omar, M. A. Monem, Y. Firouz, J. Salminen, J. Smekens, O. Hegazy, H. Gaulous, G. Mulder, P. Van den Bossche, T. Coosemans, J. Van Mierlo, "Lithium iron phosphate based battery - Assessment of the aging parameters and development of cycle life model," Appl. Energy, vol. 113, pp. 1575–1585, 2014.

[16] G. L. Plett, "Extended Kalman filtering for battery management systems of LiPB-based HEV battery packs Part 1 . Background," vol. 134, pp. 252–261, 2004.

[17] L. De Sutter, "Design , implementation and validation of live state of charge estimator based on the extended Kalman filter," 2016.

[18] O. Bohlen, J. Kowal, and D. U. Sauer, "Ageing behaviour of electrochemical double layer capacitors. Part I. Experimental study and ageing model," *J. Power Sources*, vol. 172, no. 1, pp. 468–475, 2007.

[19] M. Soltani, J. Ronsmans, S. Kakihara, J. Jaguemont, P. Van den Bossche, J. van Mierlo, N. Omar, "Hybrid Battery/Lithium-Ion Capacitor Energy Storage System for a Pure Electric Bus for an Urban Transportation Application," Appl. Sci., vol. 8, no. 7, p. 1176, 2018.